

UC Irvine

UC Irvine Previously Published Works

Title

Rapamycin and Chloroquine: The In Vitro and In Vivo Effects of Autophagy-Modifying Drugs Show Promising Results in Valosin Containing Protein Multisystem Proteinopathy

Permalink

<https://escholarship.org/uc/item/4q91t3mn>

Journal

PLOS ONE, 10(4)

ISSN

1932-6203

Authors

Nalbandian, Angèle
Llewellyn, Katrina J
Nguyen, Christopher
[et al.](#)

Publication Date

2015

DOI

10.1371/journal.pone.0122888

Peer reviewed

RESEARCH ARTICLE

Rapamycin and Chloroquine: The *In Vitro* and *In Vivo* Effects of Autophagy-Modifying Drugs Show Promising Results in Valosin Containing Protein Multisystem Proteinopathy

Angèle Nalbandian^{1,2*}, Katrina J. Llewellyn^{1,2}, Christopher Nguyen¹, Puya G. Yazdi^{2,3}, Virginia E. Kimonis^{1,2*}

1 Department of Pediatrics, Division of Genetics and Metabolism, University of California, Irvine, California, United States of America, **2** Sue and Bill Gross Stem Cell Center, University of California, Irvine, California, United States of America, **3** Systemic Health LLC, Los Angeles, California, United States of America

* a.nalbandian@uci.edu (AN); vkimonis@uci.edu (VEK)



OPEN ACCESS

Citation: Nalbandian A, Llewellyn KJ, Nguyen C, Yazdi PG, Kimonis VE (2015) Rapamycin and Chloroquine: The *In Vitro* and *In Vivo* Effects of Autophagy-Modifying Drugs Show Promising Results in Valosin Containing Protein Multisystem Proteinopathy. PLoS ONE 10(4): e0122888. doi:10.1371/journal.pone.0122888

Academic Editor: Maasaki Komatsu, The Tokyo Metropolitan Institute Medical Science, JAPAN

Received: September 2, 2014

Accepted: January 21, 2015

Published: April 17, 2015

Copyright: © 2015 Nalbandian et al. This is an open access article distributed under the terms of the [Creative Commons Attribution License](https://creativecommons.org/licenses/by/4.0/), which permits unrestricted use, distribution, and reproduction in any medium, provided the original author and source are credited.

Data Availability Statement: All relevant data are within the paper.

Funding: This work was supported by National Institutes of Health (NIH) grant R21 AR063360 and Muscular Dystrophy Association (MDA) funding 175682 to VEK. The funders had no role in study design, data collection and analysis, decision to publish, or preparation of the manuscript.

Competing Interests: Puya Yazdi is affiliated with Systemic Health, LLC based in Los Angeles, CA and

Abstract

Mutations in the valosin containing protein (VCP) gene cause hereditary Inclusion body myopathy (hIBM) associated with Paget disease of bone (PDB), frontotemporal dementia (FTD), more recently termed multisystem proteinopathy (MSP). Affected individuals exhibit scapular winging and die from progressive muscle weakness, and cardiac and respiratory failure, typically in their 40s to 50s. Histologically, patients show the presence of rimmed vacuoles and TAR DNA-binding protein 43 (TDP-43)-positive large ubiquitinated inclusion bodies in the muscles. We have generated a VCP^{R155H/+} mouse model which recapitulates the disease phenotype and impaired autophagy typically observed in patients with VCP disease. Autophagy-modifying agents, such as rapamycin and chloroquine, at pharmacological doses have previously shown to alter the autophagic flux. Herein, we report results of administration of rapamycin, a specific inhibitor of the mechanistic target of rapamycin (mTOR) signaling pathway, and chloroquine, a lysosomal inhibitor which reverses autophagy by accumulating in lysosomes, responsible for blocking autophagy in 20-month old VCP^{R155H/+} mice. Rapamycin-treated mice demonstrated significant improvement in muscle performance, quadriceps histological analysis, and rescue of ubiquitin, and TDP-43 pathology and defective autophagy as indicated by decreased protein expression levels of LC3-I/II, p62/SQSTM1, optineurin and inhibiting the mTORC1 substrates. Conversely, chloroquine-treated VCP^{R155H/+} mice revealed progressive muscle weakness, cytoplasmic accumulation of TDP-43, ubiquitin-positive inclusion bodies and increased LC3-I/II, p62/SQSTM1, and optineurin expression levels. Our in vitro patient myoblasts studies treated with rapamycin demonstrated an overall improvement in the autophagy markers. Targeting the mTOR pathway ameliorates an increasing list of disorders, and these findings suggest that VCP disease and related neurodegenerative multisystem proteinopathies can now be included as disorders that can potentially be ameliorated by rapalogs.

has no competing interests. This does not alter the authors' adherence to PLOS One policies on sharing data and materials. There are no restrictions on sharing data.

Introduction

Inclusion body myopathy (IBM) associated with Paget's disease of the bone (PDB) and Frontotemporal Dementia, (IBMPFD, MIM 167320), was first reported in 2000 by Kimonis et al. [1] and mapped to the human chromosomal region 9p13.3–12 [2] [3]. In 2004, the disease was attributed to being caused by mutations in the gene encoding *Valosin-Containing Protein (VCP)* [4]. Classic symptoms of VCP disease include weakness and atrophy of the skeletal muscles of the pelvic and shoulder girdle muscles in 90% of individuals [1–3]. Affected individuals exhibit scapular winging and die from progressive muscle weakness, and cardiac and respiratory failure, typically in their 40s to 50s [1, 5]. Histologically, patients show the presence of rimmed vacuoles and TAR DNA-binding protein 43 (TDP-43)-positive large ubiquitinated inclusion bodies in the muscles [1, 4, 5, 6]. The variable phenotype is often diagnosed as limb girdle muscular dystrophy, amyotrophic lateral sclerosis (ALS), facioscapular muscular dystrophy, or scapuloperoneal muscular dystrophy [5, 7, 8]. To date, 31 VCP mutations have been reported in families from several parts of the world, including Germany [9, 10], France [11], Austria [12], Italy [13, 14], the UK [15], Australia [16], Brazil [17], Korea [18], Japan [19] and the United States [20, 21]. Fifteen percent of individuals with hereditary inclusion body myopathy have an ALS-like phenotype and VCP mutations have been noted in 2–3% of isolated familial amyotrophic lateral sclerosis (fALS) cases [5, 22].

Autophagy plays an important role in degrading defective organelles and the bulk of cytoplasm during starvation. Impaired autophagic degradation is involved in Alzheimer's and Huntington's diseases, as well as in other neurodegenerative diseases [23–27]. Recent studies have shown that *sequestosome 1* (p62/SQSTM1) interacts with the autophagic effector protein Light Chain 3 (LC3-I/II) to mediate the autophagic uptake of aggregated proteins. VCP mutations is important for the retro-translocation of misfolded endoplasmic reticulum (ER) proteins, and mutations result in defective ER associated protein degradation (ERAD) and ER stress responses [28]. Interestingly, the *SQSTM1* gene, which encodes p62/SQSTM1, is involved in autophagy, and apoptosis, and is responsible for approximately 10% of sporadic PDB, 50% of familial PDB, as well as ALS.

We have previously generated a novel neomycin cassette-free knock-in (KI) mouse model with the common disease-related R155H VCP mutation (VCP^{R155H/+}), which has features of human VCP-associated myopathy including progressive muscle, bone, spinal cord and brain pathology. The VCP^{R155H/+} heterozygous mice demonstrate similar pathological characteristics observed in many patients, however, have a slow rate of progression [29, 30]. Double mutant VCP^{R155H/R155H} mice exhibit progressive weakness prior to their early demise as well as accelerated pathology in skeletal muscle, spinal cord, and bone [31].

Autophagy-modifying therapeutics including rapamycin and chloroquine for neuromuscular diseases is currently being evaluated. Rapamycin belongs to the class of macrocyclic immunosuppressive drugs used in preventing rejection after organ transplantation, topical treatment of facial angiofibromas, renal angiomyolipoma, brain tumors associated with tuberous sclerosis and chemotherapy for a variety of cancers. Intracellularly, rapamycin forms a complex with *FK binding protein 12 kDa (FKBP12)* and mammalian Target of Rapamycin Complex 1 (mTORC1), and blocks the pro-proliferative and anti-apoptotic signaling pathways by autophosphorylation and dissociation of mTORC1 complex and thus, blocking the binding of mTOR to its substrates. Our previous studies have shown a dysfunction in the autophagic

signaling cascade via accumulation of autophagy intermediates, such as proteins p62/SQSTM1, Light Chain LC3-I/II and optineurin in VCP^{R155H/+} and VCP^{R155H/R155H} animals versus their Wild Type (WT) littermates. Stimulation of blocked autophagy by rapamycin may enhance the impaired autophagic flux observed in VCP multisystem proteinopathies. Thus, clinically approved doses of rapamycin may prove to be a therapeutic option in patients suffering from VCP-related neuromuscular diseases. Chloroquine is a lysosomal inhibitor and has been shown to reverse autophagy by accumulating in lysosomes, disturbing the vacuolar H⁺ ATPase responsible for lysosomal acidification and blocking autophagy. Several reports have demonstrated the deleterious effects on muscle fiber regeneration, cell growth, and protein synthesis, however, its effect on inclusion body myopathy has not been previously studied. In this report, we investigated the effects of rapamycin and chloroquine administration in 18–20 month old VCP^{R155H/+} heterozygous and WT mice to assess any potential therapeutic value for patients with VCP multisystem proteinopathy.

Materials and Methods

Ethics Statement

All experiments were performed with the approval of the Institutional Animal Care and Use Committee (IACUC) of the University of California, Irvine (UCI) (Protocol #2007-2716-2), and in accordance with the guidelines established by the National Institutes of Health (NIH). WT and VCP^{R155H/+} mice were housed in the vivarium and were maintained under constant temperature (22°C) and humidity with a controlled 12:12-hour light-dark cycle. All animals (VCP^{R155H/+}, WT, including control littermates) were on a C57BL/6J genetic background [32]. All experiments performed in this study were genetically identified by genotyping (Transnetix Inc., Cordova, TN). Animals were observed throughout the entire experimental process in order to ameliorate any pain and suffering. Mice were euthanized by CO₂ inhalation followed by cervical dislocation.

Animal Drug Treatments

Rapamycin. Rapamycin (Sirolimus) (Sigma-Aldrich, St. Louis, MO) is a potent immunosuppressive agent that directly binds the mTORC Complex1 (mTORC1) and inhibits the mTOR (serine/threonine protein kinase) pathway, that regulates cell growth, cell proliferation, cell motility, survival and protein synthesis. Rapamycin inhibits activation of p70S6 kinase and Tor1p/Tor2p (target of rapamycin proteins), ultimately resulting in cellular responses through a translational arrest mechanism and an autophagy inducer by activating the initiation stage. The mTOR pathway is dysregulated in several human diseases. Thus, to examine the effects of rapamycin, we treated 18–20 month old WT (n = 10) and VCP^{R155H/+} (n = 10) knock-in mice with a dose of 3mg/kg body weight rapamycin, three times a week for 8 weeks by IP administration. The half-life of rapamycin is 58–63 hours (~ 3 days).

Chloroquine. Chloroquine (Sigma-Aldrich, St. Louis, MO) is one of many compounds which have shown to reverse autophagy by accumulating in lysosomes, disturbing the vacuolar H⁺ ATPase, which is responsible for lysosomal acidification and blocking autophagy. Thus, to examine the effects of chloroquine, we treated 18–20 month old WT (n = 10) and VCP^{R155H/+} (n = 10) mice with a dose of 15mg/kg body weight chloroquine, daily by subcutaneous injections for 8 weeks. The half-life of chloroquine is 30–60 days.

Measurements of weight, motor coordination and muscle strength

VCP^{R155H/+} or WT mice (n = 10, 18–20 month old males) were placed on the Rotarod, which accelerates from 4 to 40 rpm in 5 minutes. The results were recorded as the time it took for a mouse to drop down from the Rotarod for the first time. Mice went through three trials with 45- to 60-minute inter-trial intervals on each of two consecutive days. Data from the previous two-day trial were used to set the baseline. Statistical analyses were performed by student's *t*-test.

Biochemical Analyses

Hematoxylin and Eosin. Samples of quadriceps muscle from VCP^{R155H/+} (n = 10) and WT (n = 10) mice were fixed in 10% neutral-buffered formalin and stored at -80°C before sectioning at 10µm. Hematoxylin and Eosin (H&E) staining was performed using routine methods and analyzed by light microscopy (Carl Zeiss, Thornwood, NY) (Magnification 40X).

Immunohistochemistry

Quadriceps muscle samples from rapamycin- or chloroquine-treated 18–20 month old wild-type (n = 10) and VCP^{R155H/+} (n = 10) knock-in mice were harvested and embedded in cryosectioning mounting media (Electron Microscopy Sciences, Hatfield, PA), and stored at -80°C before sectioning at 5–10µm. For immunohistochemical analyses, sections were incubated Light chain 3 (LC3-I/II) (Novus Biologicals, Littleton, CO), p62/SQSTM1, mTOR signaling intermediate substrates (mTOR, p70S6K), optineurin (OPN), ubiquitin (Biomol, Plymouth Meeting, PA), TDP-43 (Abcam, Cambridge, MA), and VCP (Affinity BioReagents, Golden, CO) overnight in a humidified chamber. Subsequently, sections were washed with TBST (0.5%) and incubated with fluorescein-conjugated secondary antibodies (Sigma-Aldrich, St. Louis, MO) for 1 hour at room temperature and mounted with DAPI-containing mounting media (Vector Laboratories, Inc., Burlingame, CA). Sections were analyzed by fluorescence microscopy using an AxioVision image capture system (Carl Zeiss, Thornwood, NY).

Immunoblotting

Quadriceps muscle samples (n = 10) from rapamycin- and chloroquine-treated 18–20 month old wild-type and VCP^{R155H/+} knock-in mice were harvested and extracted using the NE-PER Nuclear and Cytoplasmic Extraction Kit (Thermo Scientific, Rockford, IL). Protein concentrations were determined using the Nanodrop according to the manufacturer's protocols. Equal amount of proteins were separated on Bis-Tris 4–12% NuPAGE gels according to manufacturer's protocols. The expression levels of proteins were analyzed by Western blotting using LC3-I/II (Novus Biologicals, Littleton, CO), p62/SQSTM1, mTOR substrates, ubiquitin, optineurin, VCP, and TDP-43 primary antibodies (Abcam, Cambridge, MA). Equal protein loading was confirmed by β actin antibody (Santa Cruz Biotechnology, Santa Cruz, CA) staining.

TUNEL Analysis

Apoptosis in mouse quadriceps muscle tissue samples (n = 10) was analyzed by the DeadEnd Fluorometric TUNEL System (Promega, Madison, WI). For TUNEL analysis, rapamycin- and chloroquine-treated VCP patients' myoblasts and muscle cryosections from VCP^{R155H/+} mice and WT littermates were stained as described previously [32]. Briefly, cells were fixed in 4% paraformaldehyde for 15 minutes, washed in PBS for 5 minutes and permeabilized with 20µg/ml Proteinase K solution for 10 minutes at room temperature. Cells were then washed in PBS for 5 minutes and 100µl of equilibration buffer was added for 10 minutes. The cells were labeled with

50 μ l of TdT reaction mix and incubated for 60 minutes at 37°C in a humidified chamber. Stop reaction was added for 15 minutes after which the cells were washed, counterstained, and prepared for analysis. The percentage of TUNEL+ cells was calculated and plotted.

Patient *In Vitro* Treatments

This study design was approved by Institutional Review Board at University of California. Mutant patient cell line with the heterozygous R155H mutation was obtained from the Muscle Tissue Culture Collection (MTCC)/EuroBioBank (Munich, Germany) as previously described [33]. Patient VCP disease myoblasts were grown to 60% confluence cultured in DMEM supplemented with 10% FBS (PromoCell Inc., Germany) at 37°C 5% humidified incubator. Cells were seeded onto 6-well plates and treated with either 0, 1, 10, or 100 μ M concentrations of rapamycin or chloroquine for varying time points either 24 or 48 hours, respectively. Immunocytochemistry was performed according to manufacturer's instructions (Abcam, Cambridge, MA). Cell lysates were collected and subjected to western blotting for analysis of autophagy signaling pathway intermediates.

Statistical Analysis

Means were used as summary statistics for all experiments. We compared the above studies—including weights, Rotarod performance immunohistological, Western blot and *in vitro* studies—in VCP^{R155H/+} and WT mice using mixed model analysis of variance and pair-wise *t*-tests. For TUNEL+ cell analyses for patients' myoblasts, results are expressed as means \pm SEM and significance was determined using two-tailed Student's *t*-test or two-way ANOVA with Bonferroni post-test. A probability of $p < 0.05$ was considered to be significant.

Results

Rapamycin, but not chloroquine treatment significantly improves muscle strength and performance

Our VCP^{R155H/+} mouse model demonstrates progressive muscle weakness approximately at the age of 6 months with vacuolization of myofibrils and centrally located nuclei, as well as cytoplasmic accumulation of TDP-43. Thus, to determine the effects of rapamycin *in vivo*, VCP^{R155H/+} and WT animals ($n = 10$ /group) were treated with rapamycin (i.p.) at 3mg/kg/body weight and followed over a period of 8 weeks where Rotarod performance measurements were obtained at 2-week intervals. Analysis of rapamycin-treated VCP^{R155H/+} animals depicted a significantly improved performance in their latency to fall (seconds) off the Rotarod versus their untreated littermates at 2-, 4-, and 6-week intervals (Fig 1A). However, no significant trend was observed in Rotarod performance levels in the VCP^{R155H/+} animals treated with chloroquine versus their untreated littermates at 2-, 4-, and 6-week intervals (Fig 1B).

Rapamycin ameliorates muscle pathology and decreases vacuoles

The VCP^{R155H/+} mouse model demonstrates typical histopathology, and progressive accumulation of TDP-43, ubiquitin, and LC3-I/II in quadriceps, resembling the onset in humans in the 30s to 40s. To understand the effects of autophagy-modifying agents on quadriceps muscle pathology, we analyzed the 20-month old rapamycin-treated VCP^{R155H/+} and WT animals. The quadriceps from the rapamycin-treated VCP^{R155H/+} mice demonstrated an overall improvement in the number of centrally located nuclei, reduced vacuoles, and an amelioration in the quadriceps fiber size and architecture (as shown in white arrows) (Fig 1C–1F). However,

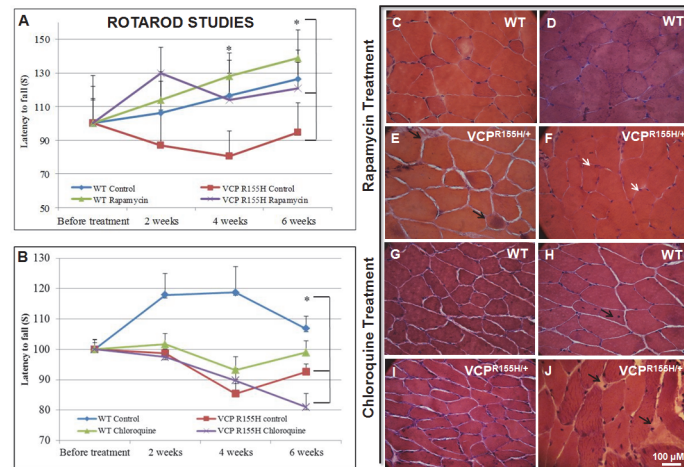


Fig 1. Rotarod performance and histological analyses of quadriceps in WT and VCP^{R155H/+} mice treated with rapamycin or chloroquine. Rotarod analysis of (A) rapamycin-treated and (B) chloroquine-treated 20-month old VCP^{R155H/+} and WT versus control animals at 2 week intervals. Histological analysis by H&E staining of quadriceps pathology from 20-month old control and (C-F) rapamycin- and (G-J) chloroquine-treated VCP^{R155H/+} and WT mice. White arrows point to overall improvement in the number of centrally located nuclei, reduced vacuoles, and an amelioration in the quadriceps fiber size and architecture. Black arrows point to worsened muscle pathology with increased vacuoles, interstitial space, and angulated fibers. The number of mice analyzed per experiment is 6–8.

doi:10.1371/journal.pone.0122888.g001

chloroquine-treated VCP^{R155H/+} mice demonstrated worsened pathology with increased vacuoles, interstitial space, and angulated fibers (as shown in black arrows) (Fig 1G–1J).

Effects of rapamycin and chloroquine on the autophagy signaling pathway

To elucidate the effects of rapamycin on the autophagy signaling pathway, we analyzed the autophagy intermediates. Autophagy flux was monitored by detection of endogenous LC3-I/II modification, ubiquitin-positive inclusions, and p62/SQSTM1 and optineurin aggregates. In comparison to the control WT and VCP^{R155H/+} mice (Fig 2A and 2B), the rapamycin-treated VCP^{R155H/+} mice demonstrated an overall decrease in ubiquitinated proteins, a decrease in LC3-I expression followed by an increased conversion to LC3-II, and a decrease in p62/SQSTM1 and optineurin (OPTN), expression levels, suggesting an improvement of the autophagic process in comparison with the rapamycin-treated animals (Fig 2C and 2D). Furthermore, we examined the TDP-43 aggregates (nuclear to cytoplasmic translocation) in the VCP^{R155H/+} animals versus their WT littermates. The rapamycin-treated VCP^{R155H/+} mice showed more nuclear TDP-43 expression, which is suggestive of a more normal phenotype. In contrast, chloroquine-treated depicted an overall increase in these autophagy intermediates (Fig 2E and 2F). Western blot of ubiquitin, TDP-43 p62/SQSTM1, LC3-I/II and OPTN confirmed these findings (Fig 2G). Distribution levels of VCP expression were comparable in quadriceps muscle of WT and VCP^{R155H/+} (data not shown).

Effects of rapamycin and chloroquine on the mTOR signaling pathway

In order to assess the effects of rapamycin on the mTOR signaling pathway, we analyzed the mTOR substrate intermediates including mTOR (7C10) and phospho-p70 S6 Kinase (Thr389) antibodies. Interestingly, immunoblotting analysis showed decreased levels of mTOR

substrates p70 and mTOR in the $VCP^{R155H/+}$ heterozygote mice treated with rapamycin whereas the protein levels of these substrates remained the same in chloroquine-treated mice (Fig 2G).

Mitochondrial complex analysis after autophagy-modifying treatments

To examine the effects of rapamycin or chloroquine administration on the mitochondrial complexes of $VCP^{R155H/+}$ and WT animals, we performed mitochondrial assays. Identification of oxidative and non-oxidative fibers is used in assessing mitochondrial pathology. Compared to 20-month old WT littermates which depicted a normal “checkered” pattern, succinic dehydrogenase (SDH) staining of heterozygous $VCP^{R155H/+}$ mice quadriceps revealed increased Type II fibers (dark fibers) oxidative fibers (Fig 3A–3F). $VCP^{R155H/+}$ heterozygous mice treated with rapamycin revealed a decrease in Type II fibers (dark fibers) suggestive of normal mitochondrial proliferation and balanced oxidative capacity (Fig 3E). Interestingly, chloroquine had no effect on the Type II fibers (Fig 3F). Quantification of oxidative fibers with autophagy-modifying drugs is shown in Fig 3M. Recently, pregnant dams and their pups fed a lipid-enriched diet (LED) resulted in the reversal of the lethal phenotype in homozygous offspring and improved survival, motor activity, muscle pathology and the autophagy cascade suggesting that lipid supplementation may be a promising therapeutic strategy for patients with VCP-associated neurodegenerative diseases [34]. Thus, we analyzed generation of lipid granules in our mice and did not note granules in WT mice by Oil Red O staining, however, the untreated heterozygous $VCP^{R155H/+}$ quadriceps muscles showed small lipid granule accumulation in a scattered pattern (as shown with black arrows) (Fig 3G–3L). Remarkably, these lipid granules were markedly

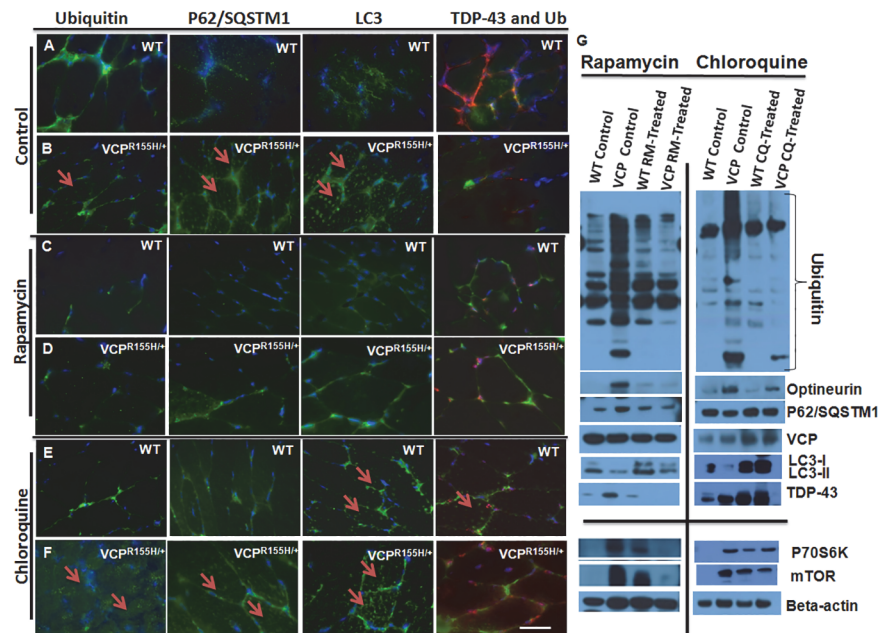


Fig 2. Immunohistochemical analyses of autophagy signaling cascade in the quadriceps of $VCP^{R155H/+}$ and WT mice treated with autophagy-modifying drugs. Quadriceps muscles from (A,B) control, (C,D) rapamycin- and (E,F) chloroquine-treated 20-month old WT and $VCP^{R155H/+}$ mice were stained with anti-ubiquitin, p62/SQSTM1, LC3-I/II, and TDP-43/ubiquitin specific antibodies, respectively (shown by arrows). Cells’ nuclei were stained with DAPI (Magnification: 630X). Scale bar represents 100 μ M. (G) Western blot expression analysis of autophagy proteins including ubiquitin, optineurin (OPTN), p62/SQSTM1, VCP, LC3-I/II, TDP-43, and mTOR pathway proteins: mTOR and p70S6K. Beta actin was used as a positive control. The number of mice analyzed per experiment is 6–8.

doi:10.1371/journal.pone.0122888.g002

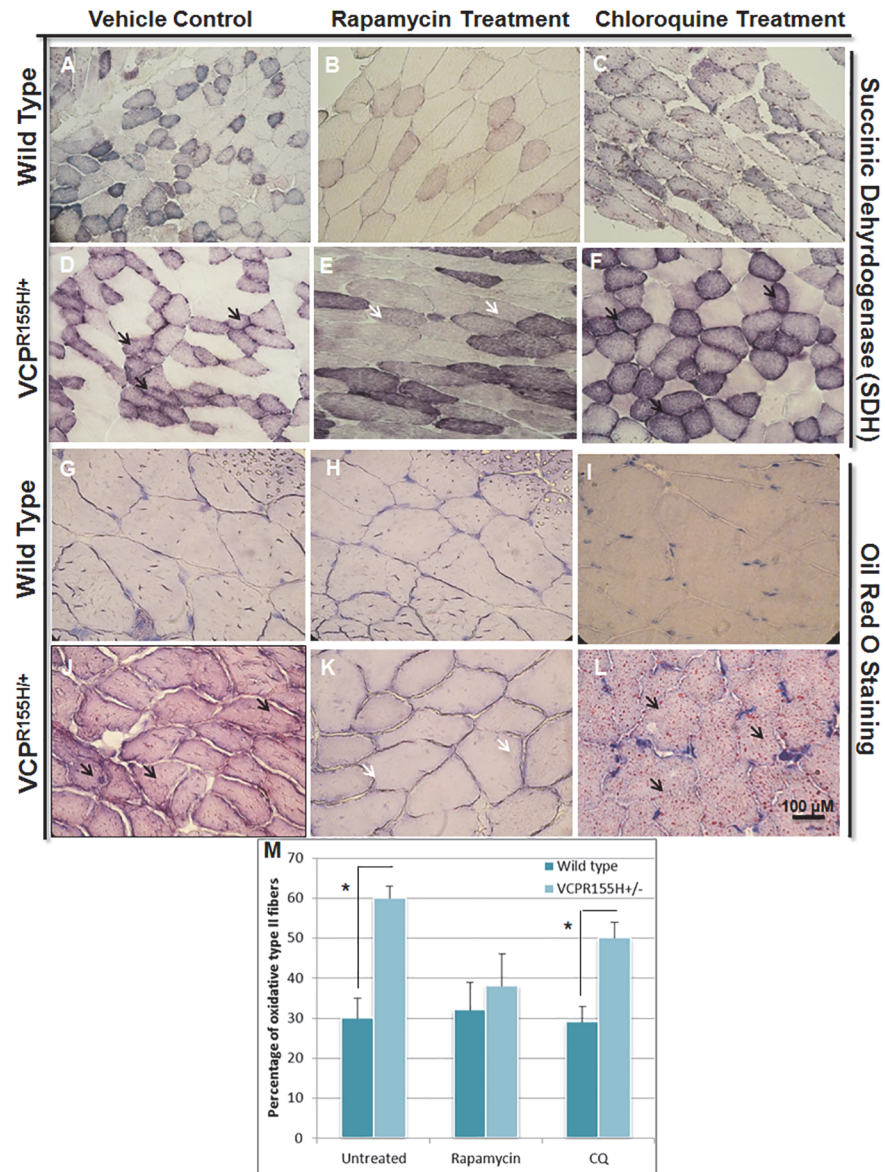


Fig 3. Mitochondrial enzyme analyses of the VCP^{R155H/+} and WT mouse quadriceps treated with rapamycin or chloroquine. Quadriceps muscles from (A,D) vehicle control (B,E) rapamycin-treated or (C,F) chloroquine-treated animals were stained with SDH antibody to observe mitochondrial proliferation and oxidative fibers/capacity (Black arrows point to Type II dark fibers; White arrows point to lighter fibers) and (G-L) Oil Red O to observe lipid droplets in WT and VCP^{R155H/+} mice at 20 months of age (Magnification: 400X). Black arrows point to increased Oil Red O Staining; white arrows point to diminished Oil Red O staining. (M) Quantification of Type II oxidative fibers with autophagy-modifying drugs. The number of mice analyzed per experiment is 8–10. Statistical significance is denoted by * $p < 0.005$ by Student one-tailed t -test.

doi:10.1371/journal.pone.0122888.g003

reduced in the VCP^{R155H/+} mice treated with rapamycin (as shown with white arrows) (Fig 3K). Conversely, chloroquine treatment resulted in an accumulation of these lipid particles in the quadriceps muscles (as indicated with black arrows) (Fig 3L).

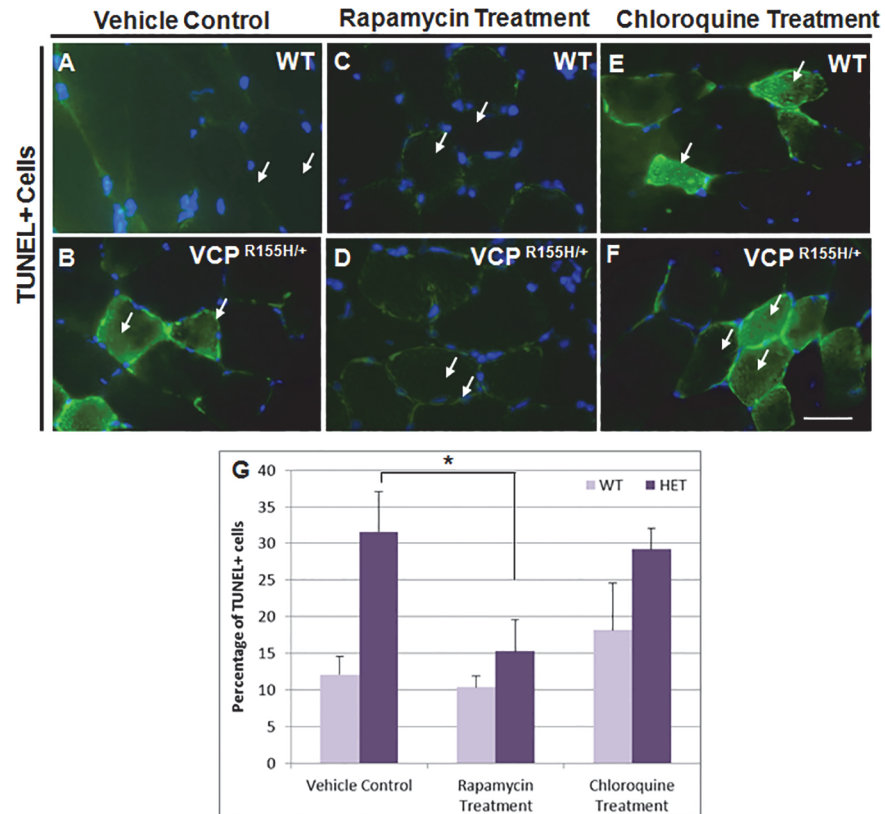


Fig 4. TUNEL analyses of quadriceps in rapamycin- and chloroquine-treated VCP^{R155H/+} and WT mice. TUNEL staining of quadriceps muscles from (A,B) control untreated (C,D) rapamycin-treated and (E,F) chloroquine-treated WT and VCP^{R155H/+} animals at 20 months of age. (G) Quantification of TUNEL+ cells in control and treated VCP^{R155H/+} and WT animals. Arrows point to TUNEL+ cells indicating cell death. Statistical significance is denoted by **p*<0.005 by Student one-tailed *t*-test. The number of animals used was *n* = 8-10/group.

doi:10.1371/journal.pone.0122888.g004

Effects of rapamycin and chloroquine on apoptosis signaling pathway

To examine the effect of autophagy-modifying drugs on apoptosis, terminal deoxynucleotidyl transferase dUTP nick end labeling (TUNEL) staining was performed on the quadriceps sections of treated and control WT and VCP^{R155H/+} mice. Rapamycin-treated muscle fibers of the VCP^{R155H/+} mice displayed reduced levels of apoptosis, as there were significantly fewer TUNEL positive cells as compared to WT littermates (Fig 4A–4D). However, no difference was observed in cell death in the chloroquine-treated WT and VCP^{R155H/+} quadriceps (Fig 4A, 4B, 4E, and 4F) as compared to untreated control littermates. Quantification of TUNEL+ cells depicting 12% cell death in vehicle control WT, 31% in vehicle control VCP^{R155H/+}, 10% in WT and 15% in rapamycin-treated mice, and 18% in WT and 29% in VCP^{R155H/+} chloroquine-treated mice (Fig 4G). Statistical significance (*p*<0.005) was observed between the control VCP^{R155H/+} and rapamycin-treated VCP^{R155H/+} mice (Fig 4G).

In vitro rapamycin treatment shows improvement in the autophagy signaling and decreases apoptosis

Previous studies by our group have demonstrated VCP mutations in patient myoblasts causing abnormal vacuolization, autophagy and cell fusion, and increased apoptosis. To explore the *in*

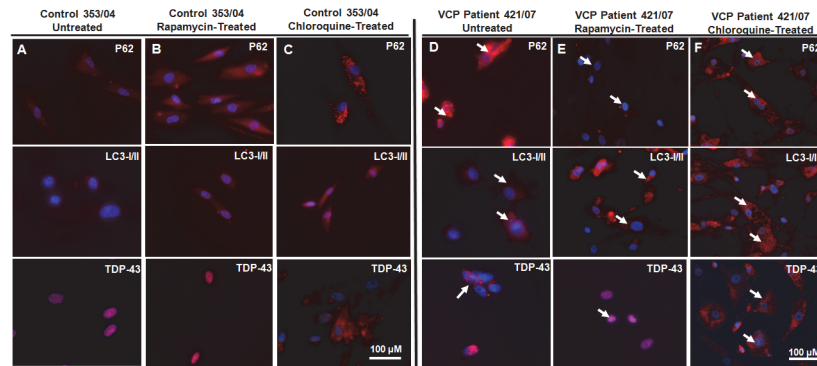


Fig 5. Immunohistochemical analyses of autophagy signaling cascade in the patients' myoblasts with VCP disease treated with either rapamycin or chloroquine. Control 353/04 (A) untreated, (B) 10μM rapamycin-treated myoblasts, (C) 10μM chloroquine-treated myoblasts stained with p62/SQSTM1 (upper panel), LC3-I/II (middle panel) and TDP-43 (lower panel) antibodies for 24 hours. VCP patient 421/07 (D) untreated (white arrows represent increased p62/SQSTM1, LC3-I/II and mislocalized TDP-43), (E) 10μM rapamycin-treated myoblasts (arrows indicated decreased expression levels of p62/SQSTM1, LC3-I/II and nuclear TDP-43), (F) 10μM chloroquine-treated (white arrows represent increased p62/SQSTM1, LC3-I/II and mislocalized TDP-43) myoblasts stained with p62/SQSTM1 (upper panel), LC3-I/II (middle panel) and TDP-43 (lower panel) antibodies for 24 hours. Scale bar represents 100 μM. Data represents triplicate studies.

doi:10.1371/journal.pone.0122888.g005

vitro effects of rapamycin and chloroquine, we treated VCP patient myoblasts (421/07) with 10μM rapamycin and stained with p62/SQSTM1 (upper panel), LC3-I/II (middle panel), and TDP-43 (lower panel) antibodies for 24 hours (Fig 5E). Similarly, we treated VCP patient myoblasts (421/07) with chloroquine and stained with p62/SQSTM1 (upper panel), LC3-I/II (middle panel), and TDP-43 (lower panel) antibodies for 24 hours (Fig 5F). Arrows point to increased expression levels of p62/SQSTM1, LC3-I/II, and TDP-43 (Fig 5D–5F). Overall, rapamycin treatment showed an improvement in the autophagy markers p62/SQSTM1 and LC3-I/II (Fig 5E), while myoblasts treated with chloroquine depicted an increased expression (Fig 5F) of autophagy markers as compared to controls (Fig 5A–5C).

In vitro rapamycin treatment decreases apoptosis in patient myoblasts

To determine apoptosis in control and patient myoblasts upon treatments with autophagy-modifying drugs, we performed TUNEL assays (Fig 6). Control 353/04 myoblasts did not show any significant differences under untreated or rapamycin-treated conditions, however, showed increased cell death after chloroquine treatment (Fig 6A–6C). Remarkably, there were fewer TUNEL+ cells after rapamycin treatment in VCP patients' 421/07 myoblasts as compared to increased cell death after chloroquine treatment (Fig 6D–6F). Quantification of TUNEL staining after autophagy-modifying treatments in control versus VCP patients' myoblasts (Fig 6G).

Discussion and Conclusions

Currently, intense investigations are underway to determine the underlying cellular and molecular disease mechanisms for the development of effective novel advancements/therapeutics of VCP-associated disease and related neurodegenerative disorders. VCP multisystem proteinopathy (MSP) is a degenerative disease which affects various systems and is involved in a number of cellular functions, most of which are related to autophagy ubiquitin-proteasome-dependent proteolysis and mitochondrial degradation [35–39]. VCP is highly conserved in evolution suggesting an essential role for normal cellular functions in both unicellular (yeast) and multi-cellular organisms [40–42]. The finding that inhibition of VCP expression promotes

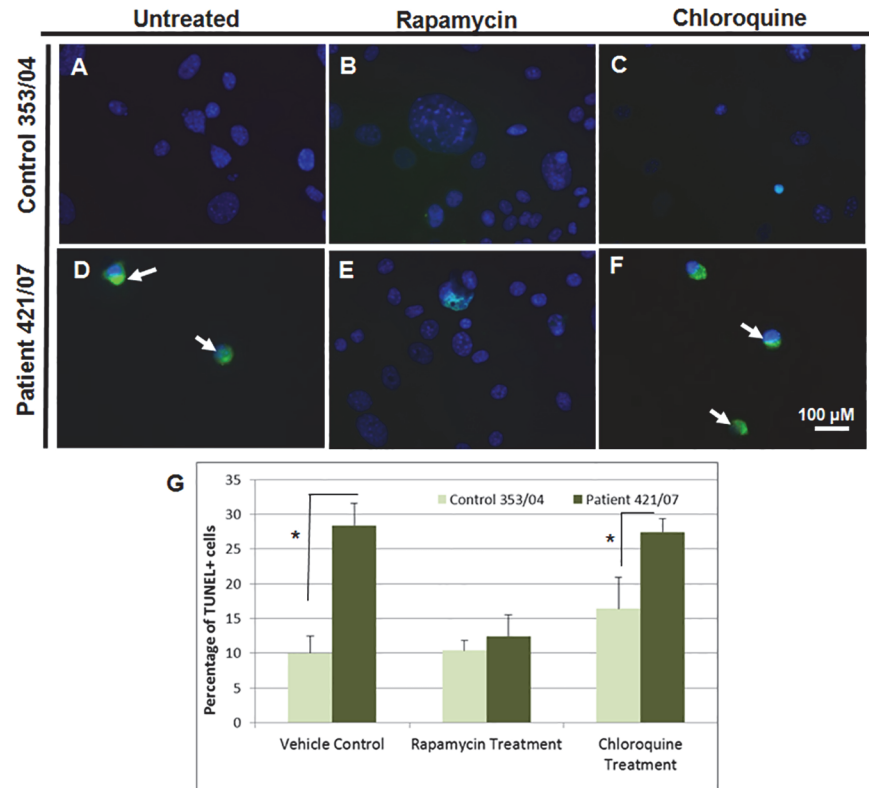


Fig 6. TUNEL analyses of autophagy signaling cascade in the patients' myoblasts with VCP disease treated with either rapamycin or chloroquine. Control 353/04 subjects' myoblasts (A) untreated, (B) 10µM rapamycin-treated and (C) 10µM chloroquine-treated stained with TUNEL. VCP patients' 421/07 myoblasts (D) untreated, (E) 10µM rapamycin-treated and (F) 10µM chloroquine-treated stained with TUNEL. Scale bar represents 100 µM. Data represents triplicate studies. (G) Percentage of TUNEL+ cells in untreated, rapamycin- and chloroquine-treated control and VCP patients' myoblasts. Data represents triplicate studies. Statistical significance is denoted by * $p < 0.005$ by Student one-tailed t -test.

doi:10.1371/journal.pone.0122888.g006

apoptosis, suggests that intact VCP is indispensable for normal development and cell survival [43]. Previous studies have confirmed the role of VCP in autophagic degradation of ubiquitinated proteins [33, 44–46]. Ching et al. (2013) demonstrated mTOR dysfunction and its contribution to vacuolar pathology and weakness in VCP inclusion body myopathy [47]. In this report, we established that rapamycin administration ameliorated the muscle pathology phenotype in the VCP^{R155H/+} animals, while chloroquine revealed a detrimental effect. Our findings further confirm a link between the autophagy-modifying treatment (rapamycin) and autophagy/cellular homeostasis. Thus, we hypothesize that rapamycin counterbalances the muscle pathology and autophagy signaling transduction pathway via the mTOR cascade and may provide a promising strategy for patients with these debilitating VCP-associated multisystem diseases.

Rapamycin is a mammalian target of rapamycin (mTOR) inhibitor-based drug with multiple uses such as in immunosuppression [48], cell proliferation and autophagy stimulation [49]. mTOR functions as an ATP and amino acid sensor to balance nutrient availability and cell growth. The mechanism of action for rapamycin occurs through binding with the 12 kDa FK506-binding protein which in turn binds and activates mTORC1 (complex 1). There has been significant progress in understanding the complexity of mTORC1 regulation over the last two decades. Dysregulation of the mTORC1 signaling pathway leads to cancers, genetic

disorders, and other age-related diseases. Autophagy-modifying agents (mTOR inhibitors) such as rapamycin (Sirolimus) provide a powerful therapeutic platform for several disorders including tuberous sclerosis (TSC), relapsed/refractory angiolipomas (AML), lymphangioleiomyomatosis (LAM), vascular tumors and hepatocellular carcinomas [50–52]. A number of studies have demonstrated that pharmacological mTORC1 inhibition may provide neuroprotection in numerous *in vivo* models of neurodegenerative diseases including Alzheimer's disease, Huntington's disease, Parkinson's disease among others [53, 54].

Scientific data suggests that accumulation of misfolded and aggregated proteins is a typical feature observed in these diseases, hypothesized to possibly being caused by mTORC1 dysregulation of protein synthesis and defective autophagic degradation. Therefore, rapamycin may prevent/reduce protein aggregation by suppressing protein synthesis and inducing the autophagy cascade. Moreover, published work by Palma et al. (2012) suggests that autophagy reactivation is therapeutic in mdx mouse model of dystrophy [55] and Johnson et al. (2013) demonstrated that rapamycin improves survival and ameliorates disease progression in the *Ndufs4*^{-/-} mouse model of Leigh syndrome [56]. Rapamycin has also demonstrated lifespan longevity in aged genetically heterogeneous mice by reducing TOR function [57], initially evidenced from studies in yeast [58, 59] and invertebrates [60].

The heterozygous VCP^{R155H/+} model of VCP-associated multisystem proteinopathy depicts pathology of the muscle, bone, brain and spinal cord, and impaired autophagy at 15 months of age [61]. In this study, we investigated the effects of autophagy-modifying agents on muscle strength, Rotarod performance, pathology, and biochemical analysis of the autophagy signaling intermediates. We found that the rapamycin-treated animals depicted an overall improvement in these parameters, while the chloroquine-treated mice displayed an exacerbation of skeletal muscle pathology and autophagy flux. As an antimalarial drug, one of the known side effects of chloroquine is muscle impairment [62]. Interestingly, a study by Jiang D. et al. (2014) demonstrated the beneficial role of exercise on the detrimental effects of chloroquine on skeletal muscles in mice was by restoring the autophagic flux [63]. However, very little research has focused on the relationship between autophagy-modifying agents, autophagy regulation, exercise physiology, and skeletal muscle mass. Remarkably, the type II fibers (dark fibers) in the mutant muscles also increased in response to rapamycin treatment, suggestive of mitochondrial proliferation and balanced oxidative capacity. Moreover, one of the major effects seen in VCP^{R155H/+} animals is lipid accumulation in their skeletal muscles, possibly be due to an imbalance between energy intake and expenditure caused by several signaling pathways. However, with rapamycin, lipid accumulation was significantly decreased in these mice, suggesting a possibly role for the involvement of mTOR mechanism. Further studies are needed to focus on these specific cascades and their interplay upon treatments with autophagy-modifying agents.

Aging VCP^{R155H/+} mice have shown relatively constant levels of apoptosis. In our report, we discovered that rapamycin-treated VCP^{R155H/+} depicted decreased levels of apoptosis as compared to their control VCP^{R155H/+} littermates, suggesting that rapamycin treatment may play a critical role in the apoptosis pathway. This was not the case with chloroquine administration. Additionally, our VCP patients' myoblasts depicted increased TUNEL+ upon treatment with chloroquine, but not rapamycin treatment. These studies suggest an important link between apoptotic cell death and autophagy stimulation in skeletal muscle, currently under further investigation.

In contrast to our findings, Ching et al (2013) reported that treatment with mTOR inhibitor rapamycin resulted in increased disease pathology and progressive muscle weakness in a different mouse model overexpressing the R155H VCP mutations [64]. In contrast, our VCP murine model was used for our current studies, which more closely resembles the human disease. Consistent with our findings, Bibee et al. (2014) have demonstrated rapamycin nanoparticles target

defective autophagy in *mdx* mice enhance muscle strength and cardiac function in Duchenne muscular dystrophy (DMD) [65].

Further elucidation of the importance of autophagy-modifying profiles and its connection to autophagic and metabolomic signaling transduction pathways could provide possible insights for future translational applications. The beneficial effects on the quadriceps muscle were achieved at a dose of rapamycin that conform with recommended clinical dosing. Recognized side effects of rapamycin include immune defects, weight gain, blood pressure, and glucose tolerance. Subsequent studies are underway to help understand the underlying and translational cellular and/or molecular signaling mechanisms to offer future prospects of utilizing autophagy-modifying novel drugs to treat patients with VCP and associated neurodegenerative multisystem proteinopathies.

Acknowledgments

We are extremely grateful to Kimberly Lank, Arianna Gomez, Naomi Walker, Andrew Dunningan, Jesus Magallan and Veeral Katheria for their technical assistance (University of California-Irvine, Department of Pediatrics, Division of Genetics and Genomics, Irvine, California).

Author Contributions

Conceived and designed the experiments: AN KL CN PY VEK. Performed the experiments: AN KL CN PY VEK. Analyzed the data: AN KL CN PY VEK. Contributed reagents/materials/analysis tools: AN KL CN PY VEK. Wrote the paper: AN KL CN PY VEK.

References

1. Kimonis VE, Kovach MJ, Waggoner B, Leal S, Salam A, Rimer L, et al. Clinical and molecular studies in a unique family with autosomal dominant limb-girdle muscular dystrophy and Paget disease of bone. *Genet Med*. 2000; 2(4):232–41. PMID: [11252708](#).
2. Kovach MJ, Waggoner B, Leal SM, Gelber D, Khardori R, Levenstien MA, et al. Clinical delineation and localization to chromosome 9p13.3-p12 of a unique dominant disorder in four families: hereditary inclusion body myopathy, Paget disease of bone, and frontotemporal dementia. *Molecular genetics and metabolism*. 2001; 74(4):458–75. doi: [10.1006/mgme.2001.3256](#) PMID: [11749051](#).
3. Watts GD, Thorne M, Kovach MJ, Pestronk A, Kimonis VE. Clinical and genetic heterogeneity in chromosome 9p associated hereditary inclusion body myopathy: exclusion of GNE and three other candidate genes. *Neuromuscul Disord*. 2003; 13(7–8):559–67. PMID: [12921793](#).
4. Watts GD, Wymer J, Kovach MJ, Mehta SG, Mumm S, Darvish D, et al. Inclusion body myopathy associated with Paget disease of bone and frontotemporal dementia is caused by mutant valosin-containing protein. *Nature genetics*. 2004; 36(4):377–81. PMID: [15034582](#).
5. Kimonis VE, Mehta SG, Fulchiero EC, Thomasova D, Pasquali M, Boycott K, et al. Clinical studies in familial VCP myopathy associated with Paget disease of bone and frontotemporal dementia. *American journal of medical genetics*. 2008; 146(6):745–57. PMID: [18260132](#).
6. Kimonis VE, Fulchiero E, Vesa J, Watts G. VCP disease associated with myopathy, paget disease of bone and frontotemporal dementia: Review of a unique disorder. *Biochimica et biophysica acta*. 2008. PMID: [18845250](#).
7. Kimonis V, Donkervoort S, Watts G. Inclusion Body Myopathy Associated with Paget Disease of Bone and/or Frontotemporal Dementia Gene [Review]. 2011. Available: <http://www.ncbi.nlm.nih.gov/pubmed/20301649>.
8. Kimonis VE, Watts GD. Autosomal dominant inclusion body myopathy, Paget disease of bone, and frontotemporal dementia. *Alzheimer disease and associated disorders*. 2005; 19 Suppl 1:S44–7. PMID: [16317258](#).
9. Schroder R, Watts GD, Mehta SG, Evert BO, Broich P, Fliessbach K, et al. Mutant valosin-containing protein causes a novel type of frontotemporal dementia. *Annals of neurology*. 2005; 57(3):457–61. PMID: [15732117](#).
10. Djamshidian A, Schaefer J, Haubenberger D, Stogmann E, Zimprich F, Auff E, et al. A novel mutation in the VCP gene (G157R) in a German family with inclusion-body myopathy with Paget disease of bone and frontotemporal dementia. *Muscle & nerve*. 2009; 39(3):389–91. PMID: [19208399](#).

11. Guyant-Marechal L, Laquerriere A, Duyckaerts C, Dumanchin C, Bou J, Dugny F, et al. Valosin-containing protein gene mutations: clinical and neuropathologic features. *Neurology*. 2006; 67(4):644–51. PMID: [16790606](#).
12. Haubenberger D, Bittner RE, Rauch-Shorny S, Zimprich F, Mannhalter C, Wagner L, et al. Inclusion body myopathy and Paget disease is linked to a novel mutation in the VCP gene. *Neurology*. 2005; 65(8):1304–5. PMID: [16247064](#).
13. Bersano A, Del Bo R, Lamperti C, Ghezzi S, Fagiolari G, Fortunato F, et al. Inclusion body myopathy and frontotemporal dementia caused by a novel VCP mutation. *Neurobiology of aging*. 2007. PMID: [17889967](#).
14. Viassolo V, Previtali SC, Schiatti E, Magnani G, Minetti C, Zara F, et al. Inclusion body myopathy, Paget's disease of the bone and frontotemporal dementia: recurrence of the VCP R155H mutation in an Italian family and implications for genetic counselling. *Clinical genetics*. 2008. PMID: [18341608](#).
15. Miller TD, Jackson AP, Barresi R, Smart CM, Eugenicos M, Summers D, et al. Inclusion body myopathy with Paget disease and frontotemporal dementia (IBMPFD): clinical features including sphincter disturbance in a large pedigree. *Journal of neurology, neurosurgery, and psychiatry*. 2009; 80(5):583–4. PMID: [19372299](#). doi: [10.1136/jnnp.2008.148676](#)
16. Kumar KR, Needham M, Mina K, Davis M, Brewer J, Staples C, et al. Two Australian families with inclusion-body myopathy, Paget's disease of bone and frontotemporal dementia: novel clinical and genetic findings. *Neuromuscul Disord*. 2010; 20(5):330–4. Epub 2010/03/26. doi: S0960-8966(10)00107-0 [pii] doi: [10.1016/j.nmd.2010.03.002](#) PMID: [20335036](#).
17. Fanganiello RD, Kimonis V, Nitrini R, Passos-Bueno MR. A Brazilian family with IBMPFD caused by p. R93C mutation in the VCP gene and literature review for genotype-phenotype correlations. *Experimental Brain Research—Manuscript ID EBR-10-0487* 2011.
18. Kim EJ, Park YE, Kim DS, Ahn BY, Kim HS, Chang YH, et al. Inclusion body myopathy with Paget disease of bone and frontotemporal dementia linked to VCP p.Arg155Cys in a Korean family. *Archives of neurology*. 2011; 68(6):787–96. Epub 2011/02/16. doi: archneuro.2010.376 [pii] doi: [10.1001/archneuro.2010.376](#) PMID: [21320982](#).
19. Komatsu J, Iwasa K, Yanase D, Yamada M. Inclusion body myopathy with Paget disease of the bone and frontotemporal dementia associated with a novel G156S mutation in the VCP gene. *Muscle & nerve*. 2013. doi: [10.1002/mus.23960](#) PMID: [23868359](#).
20. Spina S, Van Laar A, Murrell JR, de Courten-Myers G, Hamilton RL, Farlow MR, et al. Frontotemporal dementia associated with a Valosin-Containing Protein mutation: report of three families. *The FASEB Journal* 2008; 22: 58.4.
21. Watts GD, Thomasova D, Ramdeen SK, Fulchiero EC, Mehta SG, Drachman DA, et al. Novel VCP mutations in inclusion body myopathy associated with Paget disease of bone and frontotemporal dementia. *Clinical genetics*. 2007; 72(5):420–6. Epub 2007/10/16. doi: CGE887 [pii] doi: [10.1111/j.1399-0004.2007.00887.x](#) PMID: [17935506](#).
22. Johnson JO, Mandrioli J, Benatar M, Abramzon Y, Van Deerlin VM, Trojanowski JQ, et al. Exome sequencing reveals VCP mutations as a cause of familial ALS. *Neuron*. 2010; 68(5):857–64. Epub 2010/12/15. doi: S0896-6273(10)00978-5 [pii] doi: [10.1016/j.neuron.2010.11.036](#) PMID: [21145000](#).
23. Wong E, Cuervo AM. Autophagy gone awry in neurodegenerative diseases. *Nature neuroscience*. 13(7):805–11. PMID: [20581817](#). doi: [10.1038/nn.2575](#)
24. Komatsu M, Kominami E, Tanaka K. Autophagy and neurodegeneration. *Autophagy*. 2006; 2(4):315–7. PMID: [16874063](#).
25. Malicdan MC, Nishino I. Autophagy in lysosomal myopathies. *Brain pathology (Zurich, Switzerland)*. 2012; 22(1):82–8. Epub 2011/12/14. doi: [10.1111/j.1750-3639.2011.00543.x](#). PMID: [22150923](#).
26. Levine B, Kroemer G. Autophagy in the pathogenesis of disease. *Cell*. 2008; 132(1):27–42. Epub 2008/01/15. doi: S0092-8674(07)01685-6 [pii] doi: [10.1016/j.cell.2007.12.018](#) PMID: [18191218](#); PubMed Central PMCID: PMC2696814.
27. Tung YT, Wang BJ, Hu MK, Hsu WM, Lee H, Huang WP, et al. Autophagy: a double-edged sword in Alzheimer's disease. *J Biosci*. 2012; 37(1):157–65. Epub 2012/02/24. PMID: [22357213](#).
28. DeLaBarre B, Christianson JC, Kopito RR, Brunger AT. Central pore residues mediate the p97/VCP activity required for ERAD. *Molecular cell*. 2006; 22(4):451–62. PMID: [16713576](#).
29. Nalbandian A, Llewellyn K, Badadani M, Yin H, Nguyen C, Katheria V, et al. A Progressive Translational Mouse Model of Human VCP Disease: The VCP R155H/+ Mouse. *Muscle & nerve*. 2012;(in press).
30. Yin HZ, Nalbandian A, Hsu CI, Li S, Llewellyn KJ, Mozaffar T, et al. Slow development of ALS-like spinal cord pathology in mutant valosin-containing protein gene knock-in mice. *Cell Death Dis*. 2012; 3:e374. Epub 2012/08/18. doi: cddis2012115 [pii] doi: [10.1038/cddis.2012.115](#) PMID: [22898872](#); PubMed Central PMCID: PMC3434652.

31. Nalbandian A, Llewellyn KJ, Kitazawa M, Yin HZ, Badadani M, Khanlou N, et al. The Homozygote VCP (R155H/R155H) Mouse Model Exhibits Accelerated Human VCP-Associated Disease Pathology. *PLoS ONE*. 2012; 7(9):e46308. Epub 2012/10/03. doi: [10.1371/journal.pone.0046308](https://doi.org/10.1371/journal.pone.0046308) PONE-D-12-17339 [pii]. PMID: [23029473](https://pubmed.ncbi.nlm.nih.gov/23029473/); PubMed Central PMCID: PMC3460820.
32. Badadani M, Nalbandian A, Watts GD, Vesa J, Kitazawa M, Su H, et al. VCP associated inclusion body myopathy and paget disease of bone knock-in mouse model exhibits tissue pathology typical of human disease. *PloS one*. 2010; 5(10). PMID: [20957154](https://pubmed.ncbi.nlm.nih.gov/20957154/).
33. Vesa J, Su H, Watts GD, Krause S, Walter MC, Martin B, et al. Valosin containing protein associated inclusion body myopathy: abnormal vacuolization, autophagy and cell fusion in myoblasts. *Neuromuscul Disord*. 2009; 19(11):766–72. PMID: [19828315](https://pubmed.ncbi.nlm.nih.gov/19828315/). doi: [10.1016/j.nmd.2009.08.003](https://doi.org/10.1016/j.nmd.2009.08.003)
34. Llewellyn K NA, Kwang-Mook J, Nguyen C, Avandesian A, Mozaffar T, Piomelli D, Kimonis VE. Lipid-enriched diet rescues lethality and slows down progression in a murine model of VCP-associated disease. *Human molecular genetics*. 2013. Epub 2013.
35. Bays NW, Hampton RY. Cdc48-Ufd1-Npl4: stuck in the middle with Ub. *Curr Biol*. 2002; 12(10):R366–71. PMID: [12015140](https://pubmed.ncbi.nlm.nih.gov/12015140/).
36. Dai RM, Li CC. Valosin-containing protein is a multi-ubiquitin chain-targeting factor required in ubiquitin-proteasome degradation. *Nature cell biology*. 2001; 3(8):740–4. PMID: [11483959](https://pubmed.ncbi.nlm.nih.gov/11483959/).
37. Fu X, Ng C, Feng D, Liang C. Cdc48p is required for the cell cycle commitment point at Start via degradation of the G1-CDK inhibitor Far1p. *The Journal of cell biology*. 2003; 163(1):21–6. PMID: [14557244](https://pubmed.ncbi.nlm.nih.gov/14557244/).
38. Richly H, Rape M, Braun S, Rumpf S, Hoegge C, Jentsch S. A series of ubiquitin binding factors connects CDC48/p97 to substrate multiubiquitylation and proteasomal targeting. *Cell*. 2005; 120(1):73–84. PMID: [15652483](https://pubmed.ncbi.nlm.nih.gov/15652483/).
39. Ye Y, Meyer HH, Rapoport TA. The AAA ATPase Cdc48/p97 and its partners transport proteins from the ER into the cytosol. *Nature*. 2001; 414(6864):652–6. PMID: [11740563](https://pubmed.ncbi.nlm.nih.gov/11740563/).
40. Frohlich KU, Fries HW, Rudiger M, Erdmann R, Botstein D, Mecke D. Yeast cell cycle protein CDC48p shows full-length homology to the mammalian protein VCP and is a member of a protein family involved in secretion, peroxisome formation, and gene expression. *The Journal of cell biology*. 1991; 114(3):443–53. PMID: [1860879](https://pubmed.ncbi.nlm.nih.gov/1860879/).
41. Lamb JR, Fu V, Wirtz E, Bangs JD. Functional analysis of the trypanosomal AAA protein TbVCP with trans-dominant ATP hydrolysis mutants. *The Journal of biological chemistry*. 2001; 276(24):21512–20. PMID: [11279035](https://pubmed.ncbi.nlm.nih.gov/11279035/).
42. Leon A, McKearin D. Identification of TER94, an AAA ATPase protein, as a Bam-dependent component of the *Drosophila* fusome. *Molecular biology of the cell*. 1999; 10(11):3825–34. PMID: [10564274](https://pubmed.ncbi.nlm.nih.gov/10564274/).
43. Wojcik C, Yano M, DeMartino GN. RNA interference of valosin-containing protein (VCP/p97) reveals multiple cellular roles linked to ubiquitin/proteasome-dependent proteolysis. *Journal of cell science*. 2004; 117(Pt 2):281–92. PMID: [14657277](https://pubmed.ncbi.nlm.nih.gov/14657277/).
44. Ju JS, Fuentealba RA, Miller SE, Jackson E, Piwnicka-Worms D, Baloh RH, et al. Valosin-containing protein (VCP) is required for autophagy and is disrupted in VCP disease. *The Journal of cell biology*. 2009; 187(6):875–88. PMID: [20008565](https://pubmed.ncbi.nlm.nih.gov/20008565/). doi: [10.1083/jcb.200908115](https://doi.org/10.1083/jcb.200908115)
45. Ju JS, Miller SE, Hanson PI, Weihl CC. Impaired protein aggregate handling and clearance underlie the pathogenesis of p97/VCP-associated disease. *The Journal of biological chemistry*. 2008; 283(44):30289–99. PMID: [18715868](https://pubmed.ncbi.nlm.nih.gov/18715868/). doi: [10.1074/jbc.M805517200](https://doi.org/10.1074/jbc.M805517200)
46. Ju JS, Weihl CC. p97/VCP at the intersection of the autophagy and the ubiquitin proteasome system. *Autophagy*. 6(2). PMID: [20083896](https://pubmed.ncbi.nlm.nih.gov/20083896/).
47. Ching JK, Elizabeth SV, Ju JS, Lusk C, Pittman SK, Weihl CC. mTOR dysfunction contributes to vacuolar pathology and weakness in valosin-containing protein associated inclusion body myopathy. *Human molecular genetics*. 2013; 22(6):1167–79. doi: [10.1093/hmg/dd5524](https://doi.org/10.1093/hmg/dd5524) PMID: [23250913](https://pubmed.ncbi.nlm.nih.gov/23250913/).
48. Kawai T, Murakami S, Nishiyama H, Kishino M, Sakuda M, Fuchihata H. Diagnostic imaging for a case of maxillary myxoma with a review of the magnetic resonance images of myxoid lesions. *Oral surgery, oral medicine, oral pathology, oral radiology, and endodontics*. 1997; 84(4):449–54. PMID: [9347513](https://pubmed.ncbi.nlm.nih.gov/9347513/).
49. Li J, Kim SG, Blenis J. Rapamycin: One Drug, Many Effects. *Cell Metab*. 2014. doi: [10.1016/j.cmet.2014.01.001](https://doi.org/10.1016/j.cmet.2014.01.001) PMID: [24508508](https://pubmed.ncbi.nlm.nih.gov/24508508/).
50. Ghosh I, Arun I, Sen S, Mishra L. Metastatic perivascular epithelioid cell tumor responding to mammalian target of rapamycin inhibition. *Indian journal of medical and paediatric oncology: official journal of Indian Society of Medical & Paediatric Oncology*. 2014; 35(1):99–102. doi: [10.4103/0971-5851.133733](https://doi.org/10.4103/0971-5851.133733) PMID: [25006296](https://pubmed.ncbi.nlm.nih.gov/25006296/); PubMed Central PMCID: PMC4080675.
51. Muzic JG, Kindle SA, Tollefson MM. Successful Treatment of Subungual Fibromas of Tuberous Sclerosis With Topical Rapamycin. *JAMA dermatology*. 2014. doi: [10.1001/jamadermatol.2014.87](https://doi.org/10.1001/jamadermatol.2014.87) PMID: [24919623](https://pubmed.ncbi.nlm.nih.gov/24919623/).

52. Peng ZF, Yang L, Wang TT, Han P, Liu ZH, Wei Q. Efficacy and safety of sirolimus for renal angiomyolipoma in patients with tuberous sclerosis complex or sporadic lymphangiomyomatosis: a systematic review. *The Journal of urology*. 2014. doi: [10.1016/j.juro.2014.04.096](https://doi.org/10.1016/j.juro.2014.04.096) PMID: [24813310](https://pubmed.ncbi.nlm.nih.gov/24813310/).
53. Bove J, Martinez-Vicente M, Vila M. Fighting neurodegeneration with rapamycin: mechanistic insights. *Nature reviews Neuroscience*. 2011; 12(8):437–52. doi: [10.1038/nrn3068](https://doi.org/10.1038/nrn3068) PMID: [21772323](https://pubmed.ncbi.nlm.nih.gov/21772323/).
54. Caccamo A, De Pinto V, Messina A, Branca C, Oddo S. Genetic reduction of mammalian target of rapamycin ameliorates Alzheimer's disease-like cognitive and pathological deficits by restoring hippocampal gene expression signature. *J Neurosci*. 2014; 34(23):7988–98. doi: [10.1523/JNEUROSCI.0777-14.2014](https://doi.org/10.1523/JNEUROSCI.0777-14.2014) PMID: [24899720](https://pubmed.ncbi.nlm.nih.gov/24899720/); PubMed Central PMCID: PMC4044255.
55. De Palma C, Morisi F, Cheli S, Pambianco S, Cappello V, Vezzoli M, et al. Autophagy as a new therapeutic target in Duchenne muscular dystrophy. *Cell Death Dis*. 2012; 3:e418. doi: [10.1038/cddis.2012.159](https://doi.org/10.1038/cddis.2012.159) PMID: [23152054](https://pubmed.ncbi.nlm.nih.gov/23152054/); PubMed Central PMCID: PMC3542595.
56. Johnson SC, Yanos ME, Kayser EB, Quintana A, Sangesland M, Castanza A, et al. mTOR inhibition alleviates mitochondrial disease in a mouse model of Leigh syndrome. *Science (New York, NY)*. 2013; 342(6165):1524–8. doi: [10.1126/science.1244360](https://doi.org/10.1126/science.1244360) PMID: [24231806](https://pubmed.ncbi.nlm.nih.gov/24231806/).
57. Harrison DE, Strong R, Sharp ZD, Nelson JF, Astle CM, Flurkey K, et al. Rapamycin fed late in life extends lifespan in genetically heterogeneous mice. *Nature*. 2009; 460(7253):392–5. doi: [10.1038/nature08221](https://doi.org/10.1038/nature08221) PMID: [19587680](https://pubmed.ncbi.nlm.nih.gov/19587680/); PubMed Central PMCID: PMC2786175.
58. Kaerberlein M, Powers RW 3rd, Steffen KK, Westman EA, Hu D, Dang N, et al. Regulation of yeast replicative life span by TOR and Sch9 in response to nutrients. *Science (New York, NY)*. 2005; 310(5751):1193–6. doi: [10.1126/science.1115535](https://doi.org/10.1126/science.1115535) PMID: [16293764](https://pubmed.ncbi.nlm.nih.gov/16293764/).
59. Powers RW 3rd, Kaerberlein M, Caldwell SD, Kennedy BK, Fields S. Extension of chronological life span in yeast by decreased TOR pathway signaling. *Genes & development*. 2006; 20(2):174–84. doi: [10.1101/gad.1381406](https://doi.org/10.1101/gad.1381406) PMID: [16418483](https://pubmed.ncbi.nlm.nih.gov/16418483/); PubMed Central PMCID: PMC1356109.
60. Vellai T, Takacs-Vellai K, Zhang Y, Kovacs AL, Orosz L, Muller F. Genetics: influence of TOR kinase on lifespan in *C. elegans*. *Nature*. 2003; 426(6967):620. doi: [10.1038/426620a](https://doi.org/10.1038/426620a) PMID: [14668850](https://pubmed.ncbi.nlm.nih.gov/14668850/).
61. Nalbandian A, Llewellyn KJ, Badadani M, Yin HZ, Nguyen C, Katheria V, et al. A progressive translational mouse model of human valosin-containing protein disease: the VCP(R155H/+) mouse. *Muscle & nerve*. 2013; 47(2):260–70. doi: [10.1002/mus.23522](https://doi.org/10.1002/mus.23522) PMID: [23169451](https://pubmed.ncbi.nlm.nih.gov/23169451/); PubMed Central PMCID: PMC3556223.
62. Rodriguez-Caruncho C, Bielsa Marsol I. Antimalarials in dermatology: mechanism of action, indications, and side effects. *Actas dermo-sifilograficas*. 2014; 105(3):243–52. doi: [10.1016/j.adengl.2012.10.021](https://doi.org/10.1016/j.adengl.2012.10.021) PMID: [24656224](https://pubmed.ncbi.nlm.nih.gov/24656224/).
63. Jiang D, Chen K, Lu X, Gao HJ, Qin ZH, Lin F. Exercise ameliorates the detrimental effect of chloroquine on skeletal muscles in mice via restoring autophagy flux. *Acta pharmacologica Sinica*. 2014; 35(1):135–42. doi: [10.1038/aps.2013.144](https://doi.org/10.1038/aps.2013.144) PMID: [24335841](https://pubmed.ncbi.nlm.nih.gov/24335841/).
64. Ching JK, Weihl CC. Rapamycin-induced autophagy aggravates pathology and weakness in a mouse model of VCP-associated myopathy. *Autophagy*. 2013; 9(5):799–800. doi: [10.4161/auto.23958](https://doi.org/10.4161/auto.23958) PMID: [23439279](https://pubmed.ncbi.nlm.nih.gov/23439279/); PubMed Central PMCID: PMC3669194.
65. Bibee KP, Cheng YJ, Ching JK, Marsh JN, Li AJ, Keeling RM, et al. Rapamycin nanoparticles target defective autophagy in muscular dystrophy to enhance both strength and cardiac function. *FASEB J*. 2014; 28(5):2047–61. doi: [10.1096/fj.13-237388](https://doi.org/10.1096/fj.13-237388) PMID: [24500923](https://pubmed.ncbi.nlm.nih.gov/24500923/); PubMed Central PMCID: PMC3986846.